Visible Light-Induced Partial Oxidation of Olefins on Cr-Containing Silica with Molecular Oxygen

Yasuhiro Shiraishi,* Yugo Teshima, and Takayuki Hirai

Research Center for Solar Energy Chemistry, and Division of Chemical Engineering, Graduate School of Engineering Science, Osaka University, Toyonaka 560-8531, Japan

Received: November 25, 2005; In Final Form: January 29, 2006

Photocatalytic oxidation of olefins on Cr-containing silica with molecular oxygen by visible light irradiation (λ > 400 nm) has been investigated. Cr−SiO_2 catalyst prepared by a conventional sol−gel method, containing highly dispersed chromate species, catalyzes efficient olefin oxidation with very high selectivity for partially oxidized products (>90%), whereas semiconductor TiO_2 promotes complete decomposition (CO_2 production). The Cr−SiO_2 catalyst shows much higher activity than Cr/SiO_2 prepared by an impregnation method or Cr∝MCM-41 prepared by a templating method. ESR analysis reveals that photoirradiation of the chromate species with a tetrahedral coordination (T_d^{6+}) on Cr/SiO_2 and Cr∝MCM-41 catalysts leads to the formation of excited state T_d^{5+} species (T_d^{5+}*), while irradiation to T_d^{6+} on Cr−SiO_2 produces T_d^{4+}* species. This can be explained by a homogeneous T_d^{6+} arrangement with Si species on the Cr−SiO_2 catalyst. On the strongly reduced T_d^{4+}*, olefins are strongly attracted by an electron and/or proton donation, resulting in high oxidation activity. The Cr−SiO_2 catalyst is applicable to partial oxidation of various aliphatic and aromatic olefins with very high selectivity, and does not promote undesirable dimerization. The obtained findings suggest a potential use of Cr−SiO_2 as an efficient and recyclable heterogeneous photocatalyst for partial oxidation of olefins.

1. Introduction

Selective oxidation of olefins is one of the most important reactions in organic chemical production.[1,2] Photochemical oxidation with molecular oxygen (O_2) has attracted a great deal of attention. Among them, photocatalytic systems based on a semiconductor, titanium dioxide (TiO_2), have been studied extensively.[3−7] These systems, however, promote complete olefin oxidation (decomposition into CO_2) and require UV light for catalyst activation. Development of photocatalytic systems, capable of promoting partial oxidation of olefins by visible light irradiation (λ > 400 nm), is now the focus of attention. Frei et al. have reported that visible light irradiation to an olefin-loaded zeolite successfully promotes partial olefin oxidation with O_2.[8−10] This innovative system is, however, conducted in a gas/solid system. Development of "handy" liquid/solid photocatalytic systems driven by visible light irradiation and capable of promoting partial oxidation of olefins now has been in focus.

Recently, transition metal oxides highly dispersed on inorganic support have received a great deal of attention. This is because these species demonstrate photocatalytic activities that are quite different from those of bulk oxides.[11−14] Recent reports reveal that a silica containing highly dispersed Ti-oxide[15,16] or V-oxide[17] species promotes selective olefin oxidation with O_2; however, these systems still require UV light for catalyst activation. Meanwhile, highly dispersed Cr(VI)-oxide (chromate) species have also received much attention.[18−22] The chromate species have a ligand-to-metal charge transfer (LMCT) absorption at >400 nm and act as a visible light-driven photocatalyst: Cr-containing mesoporous silica molecular sieve (Cr∝HMS) prepared by a surfactant-templating method,[18,19] Cr-impregnated HMS (Cr/HMS) and ZSM-5 (Cr/ZSM-5)[20] promote NO decomposition and propane oxidation by visible light with O_2 in a gas/solid system. Yoshida et al. have reported that the Cr−Si binary oxide (Cr−SiO_2) prepared by a conventional sol−gel method promotes selective epoxidation of propene with O_2 by visible light.[21] However, the reaction is conducted in a gas/solid system, and the mechanism for the olefin oxidation is not described at all. Recently, we have reported that the Cr−SiO_2 catalyst promotes selective oxidation of cyclohexane (CHA) to cyclohexanone by visible light with O_2 in a liquid/solid system.[22] This system demonstrates the highest cyclohexanone selectivity among the liquid/solid photocatalytic systems proposed so far. We also found that the chromate species on the Cr−SiO_2 catalyst show unexpectedly high photocatalytic activity; chromate species on the other catalysts, such as Cr/SiO_2 prepared by an impregnation method and Cr∝MCM-41 prepared by a templating method, show much lower activity. The results led to a new finding that photocatalytic activities of the chromate species depend strongly on the local environment around the species, derived from the method of the catalyst synthesis.

In the present work, photocatalytic oxidation of various olefins on Cr−SiO_2 with O_2 in a liquid/solid system has been investigated by visible light irradiation. The catalytic activity and product selectivity have been compared to those of Cr/SiO_2 and Cr∝MCM-41 catalysts. We found that Cr−SiO_2 promotes partial oxidation of various olefins with very high selectivity and shows much higher activity than the other catalysts. We describe here the catalytic role of the photoactivated chromate species on Cr−SiO_2 as determined by ESR measurements, and the fine performance of the catalyst as an efficient and recyclable heterogeneous photocatalyst for olefin oxidation.

* To whom correspondence should be addressed. E-mail: shiraish@cheng.es.osaka-u.ac.jp. Fax: +81-6-6850-6273. Phone: +81-6-6850-6271.

10.1021/jp056845k CCC: $33.50
Published on Web 03/03/2006

TABLE 1: Properties of Catalysts and Results of Photocatalytic Oxidation of Cyclohexene[a]

catalyst	S_{BET} (m^2/g)	light irradiated (nm)	yield (μmol) CO_2	yield (μmol) PO[e]	PO select.[f] (TON)[g]	PO product distribution (%) 		
Cr-SiO_2(0.1)	702.9	>400	1.2	17.8	98.9 (21.4)	20	14	67
		>320	2.4	22.8	98.3 (27.5)	21	20	59
Cr-SiO_2(0.5)	802.0	>400	1.8	24.7	98.8 (6.0)	23	18	60
		>320	4.2	33.7	98.0 (8.1)	24	21	55
Cr-SiO_2(1.7)	779.8	>400	2.9	33.5	98.6 (2.4)	21	11	68
		>320	5.2	41.8	98.0 (3.0)	22	19	59
Cr-SiO_2(3.1)	709.2	>400	1.8	31.4	94.6 (1.2)	17	15	67
		>320	4.6	40.9	99.1 (1.6)	20	12	68
Cr/SiO_2(0.1)	359.6	>400	0.4	12.0	99.4 (9.5)	14	21	65
Cr∝MCM-41(0.1)	925.8[d]	>400	trace	3.0	(3.6)	15	21	64
TiO_2(P-25)		>320	360.3	33.6	35.9	12	trace	88
		>320[b]	100.1	27.3	62.1	34	2	65
TPT[c]		>320	trace	9.2	(0.18)	37	17	46

[a] Catalyst 50 mg; acetonitrile 10 mL; CHE 500 μmol; O_2 1 atm; photoirradiation time 24 h. [b] Catalyst 10 mg; photoirradiation time 6 h. [c] TPT (2,4,6-triphenylpyrylium tetrafluoroborate) 50 μmol; photoirradiation time 12 h. [d] Average pore diameter 2.63 nm; pore volume 925.3 mm^3 g^{-1}. [e] Partially oxidized (PO) products. [f] [(PO products)/(PO products + (1/6)CO_2)] (ref 22). [g] [(PO product yields)/(Cr (or TPT) amount on catalyst)].

2. Experimental Section

2.1. Materials. All of the reagents used were of the highest commercial quality, which were supplied from Wako Pure Chemical Industries, Ltd. and Tokyo Kasei Co., Ltd. and used without further purification. The synthesis procedures for Cr−SiO_2, Cr/SiO_2, and Cr∝MCM-41 catalysts were described previously;[22] hence, they are only briefly described here. Four kinds of Cr−SiO_2(x) with different Cr content [x (mol %) = Cr/(Cr + Si) × 100; x = 0.1, 0.5, 1.7, and 3.1] were prepared by a hydrolysis of tetraethyl orthosilicate (TEOS) and $Cr(NO_3)_3$·$9H_2O$ in ethylene glycol followed by calcination. Cr/SiO_2(0.1) was prepared by stirring an amorphous silica and $Cr(NO_3)_3$·$9H_2O$ in water followed by calcination. Cr∝MCM-41(0.1) was prepared by an addition of water containing fumed silica and $CrCl_3$·$6H_2O$ to an aqueous solution (pH 11.5) containing tetraethylammonium hydroxide and cethyltrimethylammonium bromide followed by calcination. The properties of these catalysts are summarized in Table 1.

2.2. Photoreaction Procedure. Each catalyst (50 mg) was suspended in dry acetonitrile (10 mL) containing an individual olefin (500 μmol) within a Pyrex glass tube (20 cm^3; ϕ 10 mm), and each tube was sealed with a rubber septum cap. O_2 was bubbled through the solution for 5 min at 228 K to avoid the evaporation of solvent and substrates. The samples were photoirradiated by a Xe lamp (2 kW; Ushio Inc.),[22,23] filtered through an aqueous $NaNO_2$ (3 wt %) or $CuSO_4$ (10 wt %) solution, to give light wavelengths of λ > 400 or 320 nm, respectively, with magnetic stirring. The light intensities[23] are 16.0 (at 400−530 nm; through the $NaNO_2$ filter) and 25.1 mW m^{-2} (at 320−530 nm; through the $CuSO_4$ filter). The temperature of the solution during photoirradiation is 313 K. After photoirradiation, the resulting solution was recovered by centrifugation, and the concentrations of substrates and products were determined by GC-FID (Shimadzu; GC-1700) and GC-TCD (Shimadzu; GC-8A), where the product identifications were made by GC-MS (Shimadzu; GCMS-QP5050A).

2.3. Measurements. ESR spectra were recorded at the X-band with a Bruker EMX-10/12 spectrometer with a 100 kHz magnetic field modulation at a microwave power level of 1.0 mW,[24,25] where microwave power saturation of the signals does not occur. The magnetic field was calibrated with 1,1′-diphenyl-2-picrylhydrazyl (DPPH) as standard. Catalyst (50 mg) was placed in a quartz ESR tube and treated with 100 Torr of O_2 (1 Torr = 133.3 Pa) at 673 K for 1 h. The tube was then evacuated at 473 K for 2 h and cooled to room temperature. The required quantity of O_2 or olefin was then introduced to the tube. The tube was placed on an ESR sample cavity and photoirradiated at 77 K with a 500 W Xe lamp (USHIO Inc.). After photoirradiation for 0.5 h, measurement was started with continued photoirradiation. The total Cr content of the catalyst was determined by an inductively coupled argon plasma atomic emission spectrophotometer (Nippon Jarrell-Ash; ICAP575 Mark II). BET surface area and pore size distribution of the catalysts were determined by N_2 adsorption−desorption measurement at 77 K, using a BELSORP 18PLUS-SP analyzer (BEL Japan, Inc.). Diffuse reflectance UV−vis spectra of the catalysts were measured on a UV−vis spectrophotometer (Jasco Corp.; V-550 with Integrated Sphere Apparatus ISV-469) with $BaSO_4$ as reference.

3. Results and Discussion

3.1. Photocatalytic Activity. Photocatalytic oxidation of cyclohexene (CHE) was studied first with Cr−SiO_2 catalysts. Table 1 summarizes the yields of CO_2 and partially oxidized (PO) products [epoxycyclohexane (epoxyCHA), CHE-2-ol, and CHE-2-one] obtained by >400 and >320 nm irradiation conditions. The results demonstrate that all four Cr−SiO_2 catalysts promote CHE oxidation by both >320 and >400 nm

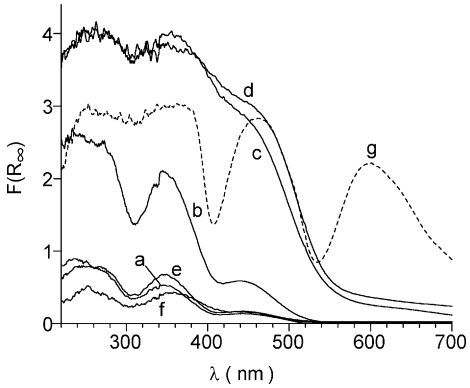

Figure 1. Diffuse reflectance UV−vis spectra of catalysts: (a) Cr−SiO_2(0.1), (b) Cr−SiO_2(0.5), (c) Cr−SiO_2(1.7), (d) Cr−SiO_2(3.1), (e) Cr/SiO_2(0.1), (f) Cr∝MCM-41(0.1), and (g) Cr_2O_3.

irradiation, indicating that these are active for visible light-induced olefin oxidation. At both irradiation conditions, Cr−SiO_2(1.7) shows higher product yield (CO_2 + PO products) than Cr−SiO_2(0.1) and Cr−SiO_2(0.5) of lower Cr content, but Cr−SiO_2(3.1) of higher Cr content shows lower yields. All four Cr−SiO_2 catalysts show similar PO product selectivity (>94%) and also similar PO product distributions at both >320 and >400 nm irradiation, indicating that Cr content on the catalysts does not affect the PO product selectivity and distribution. As shown in Table 1, turnover number (TON) for PO product formation [(PO product yields)/(Cr amount on catalyst)] on all four catalysts exceeds 1, indicating that partial oxidation of CHE proceeds catalytically even by visible light. The TON value, however, depends strongly on Cr content of the catalyst: Cr−SiO_2(0.1) shows the highest value (>20) and TON decreases with an increase in Cr content of the catalyst. This tendency is also observed for cyclohexane (CHA) photooxidation.[22]

Figure 1 summarizes diffuse reflectance UV−vis spectra of the catalysts. Cr−SiO_2(0.1) and Cr−SiO_2(0.5) show three distinctive absorption bands centered at 245, 330, and 460 nm,[22] assigned to LMCT (from O^{2-} to Cr^{6+} charge transfer) transitions of chromate species, which are highly dispersed on silica matrixes and isolated from each other.[26,27] In contrast, Cr−SiO_2(1.7) and Cr−SiO_2(3.1) show red-shifted absorption at 500−800 nm, assigned to the d−d transition of octahedral Cr^{3+} in the Cr_2O_3 cluster,[26,27] indicating that these two catalysts contain polymerized Cr^{3+} species. Use of Cr_2O_3 as a catalyst does not promote CHE oxidation, suggesting that polymerized Cr^{3+} species are inactive for CHE oxidation as well as for CHA oxidation.[22] The low activity of Cr−SiO_2 with higher Cr content (Table 1) is therefore attributable to the formation of Cr^{3+} species on the catalysts. The above findings indicate that the isolated chromate species act as the active site for CHE oxidation as well as for CHA oxidation.

A notable feature of the Cr−SiO_2 catalysts is the very high selectivity for PO products. As shown in Table 1, TiO_2 used as catalyst with UV light shows only 36% PO product selectivity, while Cr−SiO_2 when activated by both UV and visible light shows much higher selectivity (>95%), indicating that Cr−SiO_2 can suppress complete oxidation of CHE. Figure 2 shows the change in product yields during photooxidation of CHE on Cr−SiO_2(0.1) and TiO_2 catalysts. The results clearly demonstrate that Cr−SiO_2 promotes partial oxidation of CHE selectively while suppressing CO_2 formation, although the rate of product formation is lower than that on TiO_2. Figure 3 shows the change in product yields when epoxyCHA, CHE-2-ol, or CHE-2-one is used as the starting material for reactions on Cr−SiO_2(0.1) and TiO_2 catalysts. When epoxyCHA was used, both

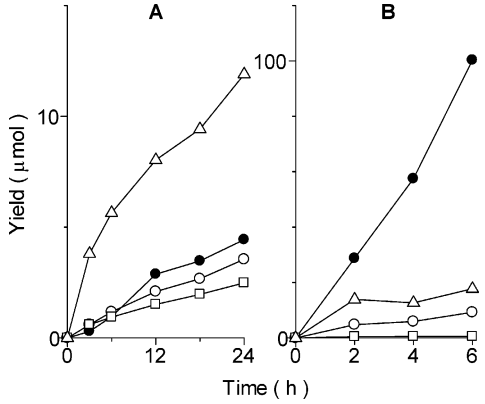

Figure 2. Change in product yields with time during photocatalytic oxidation of CHE (500 μmol) on (A) Cr−SiO_2(0.1) and (B) TiO_2: open circle, epoxyCHA; open triangle, CHE-2-one; open square, CHE-2-ol; closed circle, CO_2. Reaction conditions are as follows: (A) catalyst 50 mg, acetonitrile 10 mL, λ > 400 nm; (B) catalyst 10 mg, acetonitrile 10 mL, λ > 320 nm.

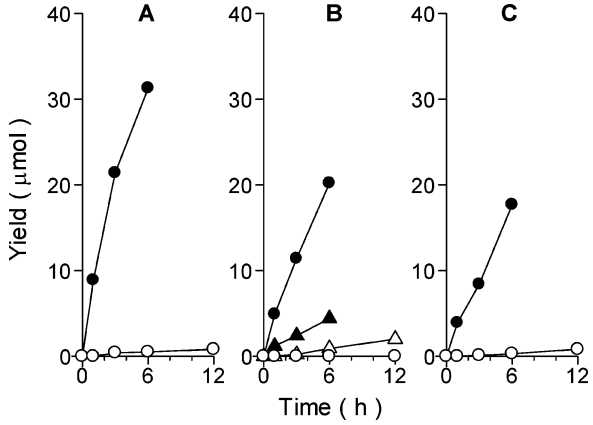

Figure 3. Change in product yields with time during reaction of (A) epoxyCHA, (B) CHE-2-ol, and (C) CHE-2-one on (open symbol) Cr−SiO_2(0.1) and (closed symbol) TiO_2: circle, CO_2; triangle, CHE-2-one. Reaction conditions are as follows: (Cr−SiO_2(0.1)) catalyst 50 mg, substrate 100 μmol, acetonitrile 10 mL, λ > 400 nm; and (TiO_2) catalyst 10 mg, substrate 100 μmol, acetonitrile 10 mL, λ > 320 nm.

catalysts promote only CO_2 formation; however, the rate of CO_2 formation on Cr−SiO_2 is much lower (one-eightieth) than that on TiO_2 (Figure 3A). Use of CHE-2-ol as the starting material affords CHE-2-one and CO_2 on TiO_2 (Figure 3B); however, Cr−SiO_2 promotes only CHE-2-one formation. Reaction of CHE-2-one on TiO_2 promotes formation of a large amount of CO_2. In contrast, the rate of CO_2 formation on Cr−SiO_2 is only one-fiftieth of that obtained on TiO_2. The above results clearly indicate that Cr−SiO_2 suppresses the sequential oxidation of PO products. This catalytic property may also enhance the partial oxidation of CHE.

3.2. Active Site Structure. Photocatalytic activity of Cr−SiO_2(0.1), prepared by a sol−gel method, was compared with that of Cr/SiO_2(0.1) and Cr∝MCM-41(0.1) prepared by other methods. The latter two catalysts have the same Cr content as Cr−SiO_2(0.1) (Table 1) and show similar absorption spectra assigned to highly dispersed chromate species (Figure 1a,e,f).[22] As summarized in Table 1, these catalysts also promote CHE oxidation by visible light irradiation, indicating that these are also effective for partial oxidation of CHE. However, the TON values for PO product formation (9.5 on Cr/SiO_2 and 3.6 on Cr∝MCM-41) are much lower than that on Cr−SiO_2 (TON 21.4). Very high TON on Cr−SiO_2 catalyst is also observed for CHA photooxidation.[22] The exceptionally high photocatalytic

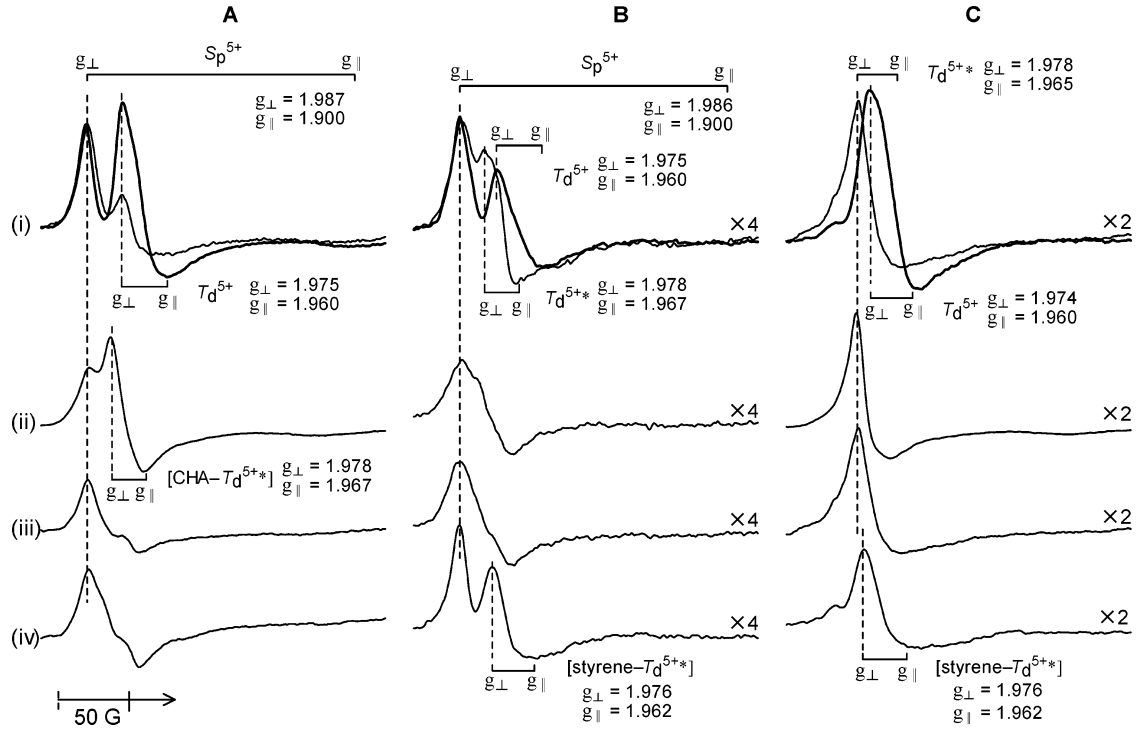

Figure 4. ESR spectra (77 K) of (A) Cr−SiO_2(0.1), (B) Cr/SiO_2(0.1), and (C) Cr∝MCM-41(0.1) catalysts, when measured (i) in vacuo (bold) without photoirradiation and (normal) with photoirradiation, (ii) with photoirradiation in the presence of 1 Torr of CHA, (iii) with photoirradiation in the presence of 1 Torr of CHE, and (iv) with photoirradiation in the presence of 1 Torr of styrene.

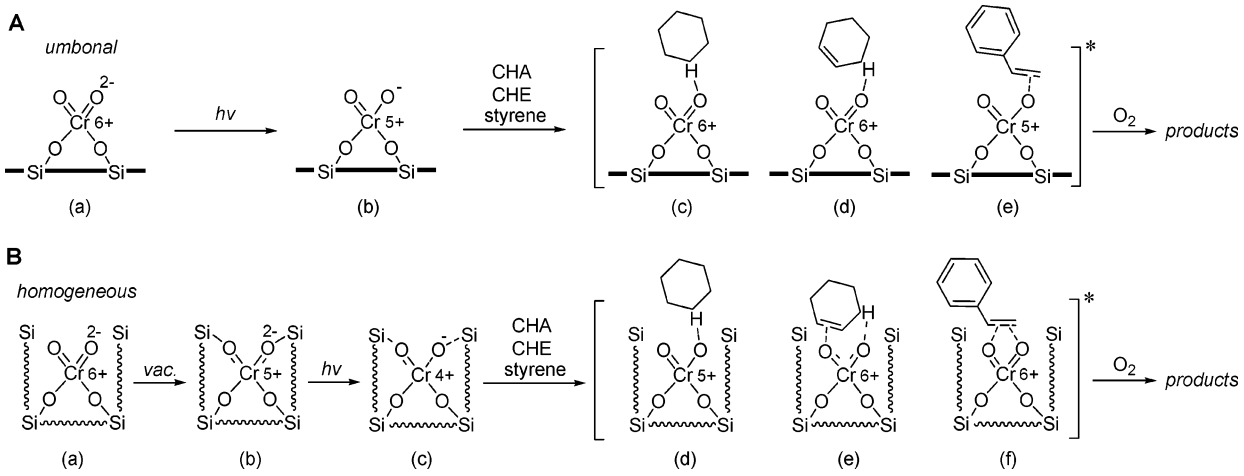

Figure 5. Schematic representation of the photocatalytic mechanism on (A) umbonal T_d^{6+} species and (B) homogeneous T_d^{6+} species.

activity is attributable to the chromate species specifically formed on Cr−SiO_2, which are derived from the method of the catalyst synthesis.[22]

Differences among the chromate species on the respective catalysts are as described previously,[22] and are summarized as follows. On a silica matrix, chromate species form tetrahedral (T_d^{6+}) and square-pyramidal (S_p^{6+}) structures.[26,27] As shown in Figure 4A−C, i (bold line), ESR spectra of Cr−SiO_2(0.1) and Cr/SiO_2(0.1) measured in vacuo at 77 K show signals assigned to the reduced T_d^{5+} and S_p^{5+} species, while Cr∝MCM-41(0.1) shows only the T_d^{5+} signal.[22] Upon photoirradiation to Cr∝MCM-41 (Figure 4C, i, normal line), the T_d^{5+} signal disappears and a new signal appears, which is assigned to the excited state T_d^{5+} species (T_d^{5+}*) formed by photoinduced charge transfer between Cr and terminal oxygen (O_T).[20,22] Photoirradiation to Cr/SiO_2 (Figure 4B, i, normal line) also leads to the T_d^{5+}* signal formation, while change in the S_p^{5+} signal is not observed. Cr−SiO_2 (Figure 4A, i, normal line) also does not show change in the S_p^{5+} signal. These findings indicate that S_p species scarcely form excited state and T_d species act as the active site. On Cr−SiO_2 (Figure 4A, i, normal line), the T_d^{5+}* signal does not appear, despite the disappearance of the T_d^{5+} signal, indicating that T_d^{5+} on Cr−SiO_2 is photoreduced to the species of lower oxidation number (Cr^{2+}, Cr^{3+}, or Cr^{4+}). A distinctive Cr^{3+} signal does not appear on the spectrum.[26,27] Cr^{2+} species are easily oxidized by O_2 to Cr^{3+};[28] however, photoirradiation to Cr−SiO_2 with O_2 (1 Torr) does not lead to Cr^{3+} signal formation. These findings indicate that the T_d^{4+}* species photoformed on Cr−SiO_2 act as the active site for photooxidation.[22]

The mechanism for the T_d^{4+}* formation on Cr−SiO_2 is explained by the differences in synthesis procedures of the catalysts.[22] In the case of Cr/SiO_2 synthesis, Cr species are impregnated on a silica surface, thus resulting in a formation of "umbonal" T_d^{6+} species on silica surface (Figure 5A, a).[19] Cr∝MCM-41 is synthesized by a simultaneous hydrolysis of $CrCl_2$ and TEOS in the presence of a surfactant template. The

rate of $CrCl_2$ hydrolysis is, however, much higher than that of TEOS,[29,30] such that Cr species rapidly surround the template micelle. Calcination of the resulting gel, therefore, also creates T_d^{6+} species with "umbonal" structure on the surface of MCM-41 mesopores. In contrast, for Cr−SiO_2 synthesis, simultaneous hydrolysis of $Cr(NO_3)_3$ and TEOS leads to the formation of a gel that arranges Cr and Si species randomly. Calcination of the resulting gel therefore creates T_d^{6+} species with a "homogeneous" structure, as depicted in Figure 5B, a. As shown in Figure 4 (A, i, bold line), the intensity of the T_d^{5+} signal on Cr−SiO_2, obtained without photoirradiation, is much higher than that on the other catalysts. The reduction of Cr^{6+} to Cr^{5+} in vacuo occurs due to a O_T−Si bond formation, associated with H_2O removal from the adjacent Si species.[26,27] On Cr−SiO_2 with homogeneous T_d^{6+}, the O_T−Si bond forms more easily than on the other catalysts with umbonal T_d^{6+} (Figure 5B, b), thus resulting in high T_d^{5+} signal intensity. On the stabilized T_d^{5+} species, photoinduced charge transfer between O_T and Cr occurs more easily, thus promoting the formation of the T_d^{4+*} species (Figure 5B, c). In contrast, on umbonal T_d^{6+} on Cr/SiO_2 and Cr∝MCM-41 catalysts, O_T−Si bond formation scarcely occurs, thus forming T_d^{5+*} species (Figure 5A, b).[12,13,19,20]

3.3. Catalytic Mechanism. The higher photocatalytic activity of the T_d^{4+*} species on Cr−SiO_2 can be explained based on the catalytic mechanism in comparison to that of the T_d^{5+*} species on the other catalysts. As described,[22] photoirradiation to all three catalysts with O_2 (1 Torr) at 77 K does not show ESR signals assigned to oxygen radicals ($O_2^{\bullet-}$, $O_3^{\bullet-}$),[16,24,25] meaning that oxygen radicals are not involved in the photocatalytic reactions occurring on T_d^{4+*} and T_d^{5+*} species. As shown in Figure 4A, ii, photoirradiation to Cr−SiO_2 with CHA (1 Torr) at 77 K does not show any signals of radical species derived from CHA,[31] but leads to an appearance of a new T_d^{5+*} signal ($g_\perp = 1.978$; $g_\parallel = 1.967$). The O_T, formed by photoinduced electron transfer, has an electrophilic character and, hence, acts as a positive hole.[32] The new T_d^{5+*} signal appearance may be attributable to a formation of a [CHA−T_d^{5+*}] complex via a proton attraction by the electrophilic O_T on T_d^{4+*} (Figure 5B, d), which may lead to oxidation of Cr^{4+} to Cr^{5+}. CHA oxidation on Cr−SiO_2 therefore proceeds via a reaction of this complex with O_2. In contrast, photoirradiation to Cr/SiO_2 and Cr∝MCM-41 with CHA shows only a decrease in the T_d^{5+*} signal (Figure 4B,C, ii), and no new signals appear. This indicates that T_d^{5+*} photoformed on these catalysts may form a [CHA−T_d^{6+*}] complex via a proton attraction, along with oxidation of Cr^{5+} to Cr^{6+} (Figure 5A, c). CHA oxidation on these catalysts proceeds via the reaction of this complex with O_2. The O_T adjacent to the highly reduced Cr^{4+} has higher electrophilicity than the O_T adjacent to Cr^{5+}. The proton attraction by more electrophilic O_T on Cr−SiO_2 is therefore much stronger than that on Cr/SiO_2 and Cr∝MCM-41, thus resulting in higher photocatalytic activity for CHA oxidation.

Figure 4B,C, iii shows ESR spectra obtained by photoirradiation to Cr/SiO_2 and Cr∝MCM-41 with CHE (1 Torr). The T_d^{5+*} signal on Cr/SiO_2 and Cr∝MCM-41 (Figure 4B,C, i, normal line) is decreased by the CHE addition, and signals derived from CHE[33] do not appear, indicating that the T_d^{5+*} on the catalysts form a [CHE−T_d^{6+*}] complex, as is also the case with CHA. When styrene, containing a terminal C═C bond but no α-proton, is added to Cr/SiO_2 and Cr∝MCM-41 samples in place of CHE (Figure 4B,C, iv), signals assigned to the styrene radical[34] do not appear, but new T_d^{5+*} signals appear. These new T_d^{5+*} signals are assigned to a [styrene−T_d^{5+*}] complex formed by interaction between the photoformed T_d^{5+*} and styrene, via an attraction of the C═C bond electron of styrene with the electrophilic O_T. This indicates that electron attraction does not change the oxidation number of Cr^{5+}. The results imply that the disappearance of the T_d^{5+*} signal ([CHE−T_d^{6+*}] complex formation) on Cr/SiO_2 and Cr∝MCM-41 by CHE addition (Figure 4B,C, iii) is attributable to the attraction of the α-proton of CHE by O_T, as is also the case with CHA (Figure 5A, c). The structures of the complexes formed between the T_d^{5+*} species and CHE or styrene can therefore be represented as in Figure 5A, d and e.

As shown in Figure 4A, iii, the ESR spectrum obtained by photoirradiation to Cr−SiO_2 with CHE shows neither a new T_d^{5+*} signal nor signals assigned to radical species derived from CHE,[16,33] indicating that the T_d^{4+*} species photoformed on Cr−SiO_2 interact with CHE to produce a [CHE−T_d^{4+*}] or [CHE−T_d^{6+*}] complex. As shown in Figure 5A, d, addition of CHE to Cr/SiO_2 and Cr∝MCM-41 leads to an oxidation of Cr^{5+} to Cr^{6+}; this suggests that T_d^{4+*} formed on Cr−SiO_2 react with CHE to form the [CHE−T_d^{6+*}] complex. The [CHE−T_d^{6+*}] complex formation between T_d^{4+*} and CHE on Cr−SiO_2 may be attributable to an attraction of the C═C bond electron of CHE with O_T, in addition to the attraction of the α-proton of CHE with O_T. The contribution of the electron attraction to the change in oxidation number of Cr may be due to the high electrophilicity of O_T on T_d^{4+*}. The complex structure can therefore be depicted in Figure 5B, e, where CHE is stabilized by both proton and electron attraction, while on Cr/SiO_2 and Cr∝MCM-41, CHE is stabilized only by proton attraction (Figure 5A, d). As shown in Table 1, the results of CHE oxidation reveal that the yield of epoxyCHA on Cr−SiO_2 is relatively higher than that on Cr/SiO_2 and Cr∝MCM-41. This indicates that the C═C bond electron of CHE is attracted more easily on Cr−SiO_2; the results support the [CHE−T_d^{6+*}] structure on Cr−SiO_2 (Figure 5B, e).

As shown in Figure 4A, iv, photoactivation of Cr−SiO_2 with styrene does not show the appearance of any signals, indicating that T_d^{4+*} on Cr−SiO_2 form a [styrene−T_d^{4+*}] or [styrene−T_d^{6+*}] complex. Considering the contribution of the attraction of the C═C bond electron of CHE to the change in oxidation number of Cr (Figure 5B, e), the T_d^{4+*} photoformed on Cr−SiO_2 may form the [styrene−T_d^{6+*}] complex (Figure 5B, f). The electron attraction of styrene by T_d^{4+*} would seem to be stronger than that by T_d^{5+*} on Cr/SiO_2 and Cr∝MCM-41 catalysts. As shown in Table 2, the photocatalytic activity of Cr−SiO_2 for styrene oxidation is much higher than that of Cr/SiO_2 and Cr∝MCM-41; the result may support the strongly attracted structure of styrene on Cr−SiO_2 (Figure 5B, f).

3.4. Photocatalytic Oxidation of Various Olefins. Table 2 summarizes the results of photooxidation of various olefins. The results demonstrate that Cr−SiO_2(0.1) promotes partial oxidation of various aliphatic and aromatic olefins catalytically (TON > 1) by visible light irradiation. The PO product selectivity for all of the olefins on Cr−SiO_2 is >90% while it is much lower on TiO_2, indicating that Cr−SiO_2 is also effective for oxidation of these olefins. The distinctive product distribution obtained on Cr−SiO_2 is as follows: reaction of linear terminal olefin (1-hexene) on Cr−SiO_2 affords pentane-1-one and 1-hexene-3-one as the major products, which are formed via C═C bond cleavage and abstraction of the α-proton, respectively, while TiO_2 affords pentane-1-one and 1,2-epoxyhexane predominantly. Reactions of styrene and α-methylstyrene on both Cr−SiO_2 and TiO_2 give the corresponding ketone as the major products. Reaction of *trans*-β-methylstyrene on Cr−SiO_2 affords benz-

TABLE 2: Results of Photocatalytic Oxidation of Various Olefins[a]

substrate catalyst	Yield (μmol) CO_2	Yield (μmol) PO	PO select[b] (TON)[c]	PO product distribution (%)			
							
Cr-SiO_2(0.1)	1.7	2.7	90.5(3.3)	20	40	40	
TiO_2	112.4	7.3	28	50	7	43	
TPT	trace	trace					
							
Cr-SiO_2(0.1)	1.7	10.3	97.3(12.4)	80		20	
Cr/SiO_2(0.1)	0.4	4.3	98.4(5.2)	78		22	
Cr∝MCM-41(0.1)	0.5	5.7	98.6(6.9)	77		23	
TiO_2	47.0	20.2	72.0	72		28	
TPT	trace	92.9[d]	(1.9)	23			
							
Cr-SiO_2(0.1)	1.8	18.3	98.4(22.0)	89	8	3	
TiO_2	114.0	72.7	79.2	91	3	6	
TPT	trace	93.8[e]	(1.9)	45			
							
Cr-SiO_2(0.1)	2.5	40.1[f]	99.0(48.3)	65	17	17	
TiO_2	36.8	47.1[f]	88.5	52	6	43	
TPT	trace	84.3[f]	(1.7)	66		19	16
					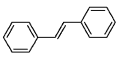	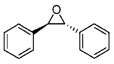	
Cr-SiO_2(0.1)[g]	1.4	38.1[f]	99.4(45.9)	4	92	4	
TiO_2[g]	32.6	39.2[f]	87.8	26	70	4	
TPT	trace	233[f]	(4.7)	10	79	1	10
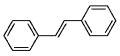						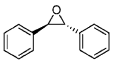	
Cr-SiO_2(0.1)[g]	1.3	85.1[f]	99.7(103)	20	69	11	
TiO_2[g]	24.2	64.9[f]	94.1	32	35	34	
TPT	trace	169[f]	(3.4)	25	57		18

[a] Reaction conditions: acetonitrile 10 mL; olefin 500 μmol; O_2 1 atm. Cr-containing silica: catalyst 50 mg; photoirradiation time 24 h (> 400 nm). TiO_2: catalyst 10 mg; photoirradiation time 6 h (> 320 nm). TPT: catalyst 50 μmol; photoirradiation time 5 h (>400 nm). [b] [(PO products)/(PO products + (1/6)CO_2)]. [c] [(PO product yields)/(Cr (or TPT) amount on catalyst)]. [d] Including dimerized products (71 μmol, 77%; see Supporting Information, Table S1). [e] Including dimerized products (52 μmol, 55%; see Supporting Information, Table S1). [f] Including isomerized products. [g] Trace amount of phenanthrene was detected (<0.5%).

aldehyde via C═C bond cleavage, with small amounts of the corresponding cis-isomer and epoxide, while TiO_2 affords ketone and epoxide mainly. Reaction of *cis*-stilbene on TiO_2 promotes trans-isomerization (70%) and ketone production (26%), but on Cr−SiO_2, trans-isomerization occurs very selectively (94%). For *trans*-stilbene, TiO_2 catalyzes cis-isomerization and formations of ketone and epoxide comparatively; however, Cr−SiO_2 promotes cis-isomerization selectively (69%).

The present Cr−SiO_2 system proceeds via an electron and/or proton attraction of olefin followed by oxidation with O_2. As is well-known, 2,4,6-triphenylpyrylium tetrafluoroborate (TPT), one of the generally used homogeneous photosensitizers, can oxidize olefins with O_2 by visible light irradiation (<470 nm).[35−40] The photoexcited TPT (TPT*) can promote electron transfer from olefin to TPT*, producing olefin cation radical (olefin$^{\bullet+}$), but does not activate O_2. The oxidation of olefin therefore proceeds via reaction of the formed olefin$^{\bullet+}$ with O_2, whose mechanism is analogous to that occurring on the present Cr−SiO_2 system. The results of olefin photooxidation by TPT are summarized in Tables 1 and 2, in comparison to that obtained by Cr−SiO_2. TPT scarcely catalyzes oxidation of aliphatic olefins, such as CHE and 1-hexene, although Cr−SiO_2 oxidizes these olefins catalytically. This is because these olefins have a more positive oxidation potential and, hence, electron transfer from olefins to TPT* is not favored thermodynamically.[35] However, on the photoactivated Cr−SiO_2, the O_T of the T_d^{4+}* species with high electrophilicity strongly attracts these olefins, thus promoting effective oxidation. For aromatic olefins with a terminal C═C bond, such as styrene and α-methylstyrene, TPT gives rise to the corresponding ketones, together with a large amount of dimerized products (>50%) (Supporting Information, Table S1). The formation of dimerized products is due to the diffusion of olefin$^{\bullet+}$. In contrast, on Cr−SiO_2, none of the dimerized products is produced during reaction. This is because these olefins are attracted strongly on the catalyst via a complex formation, thus suppressing dimerization. For aromatic olefins with internal C═C bond, such as β-methylstyrene, *cis*-stilbene, and *trans*-stilbene, TPT affords cis-/trans-isomerized products and ketones predominantly as does Cr−SiO_2, where Cr−SiO_2 shows much higher yields of isomerized products.

A notable feature of the Cr−SiO_2 catalyst is the higher turnover frequency [TOF (h^{-1}) = TON/(photoirradiation time)] for PO product formation than TPT for oxidation of all of the olefins employed. For example, with styrene, TOF values are 0.51 (Cr−SiO_2) and 0.32 h^{-1} (TPT). This suggests that *Cr−SiO_2 shows higher photocatalytic activity than TPT*, although the reaction proceeds heterogeneously. The above findings

indicate that Cr−SiO_2 has several advantages over the homogeneous TPT photosensitizer: (i) high photocatalytic activity for partial oxidation (including isomerization) of olefins; (ii) successful oxidation of aliphatic olefins; and (iii) no undesirable dimerization of olefins with a terminal C═C bond. The Cr−SiO_2 catalyst, when recovered after photoreaction, does not show decrease in the Cr content. In addition, changes in the spectra of the catalyst are not observed, and the catalyst recovered shows almost the same photocatalytic activity and PO selectivity for the olefin oxidation as the virgin Cr−SiO_2. The Cr−SiO_2 catalyst can be reused for further photoreaction and the catalyst therefore has a potential as a new visible light-driven photocatalyst for selective oxidation of olefins.

4. Conclusion

The Cr−SiO_2 catalysts containing highly dispersed chromate species have been prepared by a conventional sol−gel method. These have been employed for visible light-induced photooxidation of olefins with molecular oxygen, with the following results:

(1) Cr−SiO_2, when activated by visible light, catalyzes partial oxidation of olefins with very high selectivity, while TiO_2 promotes complete decomposition (CO_2 formation). Sequential decomposition of the PO products on Cr−SiO_2 scarcely occurs, resulting in high PO product selectivity. Cr−SiO_2 of low Cr content, which contains tetrahedrally coordinated chromate species (T_d^{6+}), demonstrates high catalytic activity. The activity of Cr−SiO_2 is much higher than that of Cr/SiO_2 and Cr∝MCM-41 catalysts prepared by other conventional methods, although the latter two also contain T_d^{6+} species.

(2) ESR measurements reveal that photoactivation of T_d^{6+} on Cr/SiO_2 and Cr∝MCM-41 catalysts leads to a formation of excited-state species (T_d^{5+*}), while photoactivation of T_d^{6+} on Cr−SiO_2 produces T_d^{4+*} species. The difference in the excited-state species is attributable to the local environment around the T_d^{6+} species. The T_d^{4+*} species formed on Cr−SiO_2 strongly attract olefins (formation of olefin−T_d complex) owing to high electrophilicity of terminal oxygen and, hence, promote efficient oxidation by molecular oxygen.

(3) The Cr−SiO_2 catalyst has several advantages over a generally used homogeneous photosensitizer, 2,4,6-triphenylpyrylium tetrafluoroborate (TPT): (i) Cr−SiO_2 catalyzes partial oxidation of aliphatic olefins, while TPT is almost inactive; (ii) Cr−SiO_2 catalyzes partial oxidation of aryl olefins with a terminal C═C bond, while TPT promotes dimerization; and (iii) Cr−SiO_2 demonstrates higher photocatalytic activity for partial oxidation of olefins than TPT. The Cr−SiO_2 recovered after reaction is recyclable without loss of catalytic activity.

Acknowledgment. We thank financial support from the Grant-in-Aid for Scientific Research (No. 15360430) and the Grant-in-Aid for Scientific Research on Priority Areas "Fundamental Science and Technology of Photofunctional Interfaces (417)" (Nos. 15033244 and 17029037) from the Ministry of Education, Culture, Sports, Science and Technology, Japan (MEXT). We are also grateful to the Division of Chemical Engineering for the Lend-Lease Laboratory System.

Supporting Information Available: Detailed product distributions in the photooxidation of styrene and α-methylstyrene (Table S1). This material is available free of charge via the Internet at http://pubs.acs.org.

References and Notes

(1) Sheldon, R. A.; Kochi, J. K. *Metal-Catalyzed Oxidation of Organic Compounds*; Academic Press: New York, 1981.
(2) Parshall, G. W.; Ittel, S. D. *Homogeneous Catalysis*, 2nd ed.; Wiley: New York, 1992.
(3) Fox, M. A.; Chen, C. *J. Am. Chem. Soc.* **1981**, *103*, 6757.
(4) Fox, M. A.; Chen, C.-C. *Tetrahedron Lett.* **1983**, *24*, 547.
(5) Kanno, T.; Oguchi, T.; Sakuragi, H.; Tokumaru, K. *Tetrahedron Lett.* **1980**, *21*, 467.
(6) Ohno, T.; Kigoshi, T.; Nakabeya, K.; Matsumura, M. *Chem. Lett.* **1998**, *27*, 877.
(7) Ohno, T.; Nakabeya, K.; Matsumura, M. *J. Catal.* **1998**, *176*, 76.
(8) Blatter, F.; Frei, H. *J. Am. Chem. Soc.* **1993**, *115*, 7501.
(9) Blatter, F.; Frei, H. *J. Am. Chem. Soc.* **1994**, *116*, 1812.
(10) Blatter, F.; Sun, H.; Vasenkov, S.; Frei, H. *Catal. Today* **1998**, *41*, 297.
(11) Maldotti, A.; Molinari, A.; Amadelli, R. *Chem. Rev.* **2002**, *102*, 3811.
(12) Anpo, M. *Photofunctional Zeolites*; Nova Science Publishers Inc: New York, 2000.
(13) Matsuoka, M.; Anpo, M. *J. Photochem. Photobiol. C* **2003**, *3*, 225.
(14) Yoshida, H.; Murata, C.; Hattori, T. *J. Catal.* **2000**, *194*, 364.
(15) Yoshida, H.; Murata, C.; Hattori, T. *Chem. Commun.* **1999**, 1551.
(16) Shiraishi, Y.; Morishita, M.; Hirai, T. *Chem. Commun.* **2005**, 5977.
(17) Amano, F.; Tanaka, T.; Funabiki, T. *Langmuir* **2004**, *20*, 4236.
(18) Yamashita, H.; Yoshizawa, K.; Ariyuki, M.; Higashimoto, S.; Che, M.; Anpo, M. *Chem. Commun.* **2001**, 435.
(19) Yamashita, H.; Ariyuki, M.; Yoshizawa, K.; Kida, K.; Ohshiro, S.; Anpo, M. *Res. Chem. Intermed.* **2004**, *30*, 235.
(20) Yamashita, H.; Ohshiro, S.; Kida, K.; Yoshizawa, K.; Anpo, M. *Res. Chem. Intermed.* **2003**, *29*, 881.
(21) Murata, C.; Yoshida, H.; Hattori, T. *Chem. Commun.* **2001**, 2412.
(22) Shiraishi, Y.; Teshima, Y.; Hirai, T. *Chem. Commun.* **2005**, 4569.
(23) Shiraishi, Y.; Koizumi, H.; Hirai, T. *J. Phys. Chem. B* **2005**, *109*, 8580.
(24) Shiraishi, Y.; Saito, N.; Hirai, T. *J. Am. Chem. Soc.* **2005**, *127*, 8304.
(25) Shiraishi, Y.; Saito, N.; Hirai, T. *J. Am. Chem. Soc.* **2005**, *127*, 12820.
(26) Weckhuysen, B. M.; Verberckmoes, A. A.; Buttiens, A. L.; Schoonheydt, R. A. *J. Phys. Chem.* **1994**, *98*, 579.
(27) Weckhuysen, B. M.; Wachs, I. E.; Schoonheydt, R. A. *Chem. Rev.* **1996**, *96*, 3327.
(28) Weckhuysen, B. M.; Schoonheydt, R. A.; Jehng, J.-M.; Wachs, I. E.; Cho, S. J.; Ryoo, R.; Kijlstra, S.; Poels, E. *J. Chem. Soc., Faraday Trans.* **1995**, *91*, 3245.
(29) Hüsing, N.; Launay, B.; Doshi, D.; Kickelbick, G. *Chem. Mater.* **2002**, *14*, 2429.
(30) Brinker, C. J.; Scherer, G. W. *Sol−Gel Science*; Academic Press: New York, 1990.
(31) Koizumi, H.; Takada, T.; Ichikawa, T.; Lund, A. *Chem. Phys. Lett.* **2001**, *340*, 256.
(32) Wada, K.; Yamada, H.; Watanabe, Y.; Mitsudo, T. *J. Chem. Soc., Faraday Trans.* **1998**, *94*, 1771.
(33) Ohnishi, S.; Nitta, I. *J. Chem. Phys.* **1963**, *39*, 2848.
(34) Bonazzola, L.; Mighaut, J.-P.; Rongin, J.; Misawa, H.; Sakuragi, H.; Tokumaru, K. *Bull. Chem. Soc. Jpn.* **1990**, *63*, 347.
(35) Miranda, M. A.; García, H. *Chem. Rev.* **1994**, *94*, 1063.
(36) Mattay, J.; Vondenhof, M.; Denig, R. *Chem. Ber.* **1989**, *122*, 951.
(37) Akaba, R.; Ohshima, K.; Kawai, Y.; Obuchi, Y.; Negishi, A.; Sakuragi, H.; Tokumaru, K. *Tetrahedron Lett.* **1991**, *32*, 109.
(38) Akaba, R.; Sakuragi, H.; Tokumaru, K. *J. Chem. Soc., Perkin Trans. 2* **1991**, *3*, 291.
(39) García, H.; Miranda, M. A.; Mojarrad, F.; Sabater, M.-J. *Tetrahedron* **1994**, *50*, 8773.
(40) Sridhar, M.; Kumar, B. A. *Chem. Lett.* **1998**, *27*, 461.